

See discussions, stats, and author profiles for this publication at: <https://www.researchgate.net/publication/257124967>

Effect of the reagent vibration on stereodynamics of the reaction $\text{Ca} + \text{HCl} \rightarrow \text{CaCl} + \text{H}$

ARTICLE *in* CHEMICAL PHYSICS · SEPTEMBER 2012

Impact Factor: 1.65 · DOI: 10.1016/j.chemphys.2012.07.010

CITATIONS

2

READS

17

5 AUTHORS, INCLUDING:

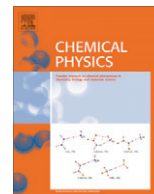


Chuan-Lu Yang

Ludong University

216 PUBLICATIONS 1,640 CITATIONS

SEE PROFILE



Effect of the reagent vibration on stereodynamics of the reaction $\text{Ca} + \text{HCl} \rightarrow \text{CaCl} + \text{H}$

Li-Zhi Wang^{a,b}, Chuan-Lu Yang^{b,*}, Jing-Juan Liang^a, Li-Li Duan^a, Qing-Qang Zhang^a

^a College of Physics and Electronics, Shandong Normal University, Jinan, Shandong 250014, China

^b School of Physics, Ludong University, Yantai 264025, China

ARTICLE INFO

Article history:

Received 21 April 2012

In final form 22 July 2012

Available online 31 July 2012

Keywords:

Vibration of reactant molecule

Vector correlation

Stereodynamics

Quasi-classical trajectory

ABSTRACT

Based on the new potential energy surface [G.Verbockhaven, C. Sanz, G.C. Groenenboom, O. Roncero, J. Chem. Phys. 122 (2005) 204307] constructed by means of the multireference configuration interaction, the influence of the reagent vibrational excitation on the $\text{Ca} + \text{HCl}$ reaction has been investigated by the quasi-classical trajectory method. The vibrational level and rotational level of the reactant molecule are taken as $v = 0-2$ and $j = 0$ respectively. The polarization-dependent generalized differential cross sections (PDDCSs) and alignments of the product rotational angular momentum for all reactions are reported. The calculation results show that the vibrational quantum number has a considerable influence on the distribution of the $\mathbf{k}-\mathbf{j}'$ vector correlation. The CaCl product mainly tends to the backward scattering for $v > 0$, the effects of initial vibrational excited state of reactant molecule on PDDCSs are also revealed.

© 2012 Elsevier B.V. All rights reserved.

1. Introduction

In recent years, the potential-energy-surface (PES) constructs and the reaction-dynamic calculations have been the subject of experimental and theoretical studies. Reaction $\text{Ca} + \text{HCl}$ that involves an alkali-earth atom and a hydrogen halide has been considered as typical “Harpoonlike” mechanism models [1] to analyze the influence of the initial state of the reactants and its effect on the final state distribution. The reactions $\text{M} + \text{HX} \rightarrow \text{MX} + \text{H}$ ($\text{M} = \text{Be}, \text{Mg}, \text{Ca}, \text{Sr}, \text{Ba}$; $\text{X} = \text{F}, \text{Cl}, \text{Br}, \text{I}$) show some interesting dynamical features, and many studies of this reaction family have been done theoretically and experimentally [2–17]. For examples, the alternative experimental study on the reaction dynamics of this system has been made by photon excitation of the Ca atom in the $\text{Ca}(\text{IS})\text{--HCl}$ van der Waals complex. However, the CaCl product was initially not detected in its electronic ground state either [18–20] because its detection is particularly difficult. Fortunately, the $\text{Ca}\text{--HCl}$ complex was detected by Visticot et al. [21] by observing the fluorescence of CaCl molecule in a supersonic beam/laser-ablation experiment. Recently, Verbockhaven et al. [22] reported a new *ab initio* PES computed using a coupled cluster method with single and double excitations and perturbative triples (CCSD(T)) and multi-reference configuration-interaction (MRCI) wave functions, this PES is reliable because the results based on the quan-

tum-dynamics calculation and the new surface are in agreement with the experimental data. Based on this PES, isotopic effects on stereodynamics for $\text{Ca} + \text{HCl}/\text{Ca} + \text{DCl}/\text{Ca} + \text{TCl}$ reactions have been successfully studied [23].

For the reaction $\text{M} + \text{HX} \rightarrow \text{MX} + \text{H}$, there are usually two processes involved. One is direct abstraction and the other is insertion. These two reaction mechanisms often play different roles in different initial situations and different reactions. In addition, this reaction family belongs to the heavy-heavy-light (HHL) mass system, which makes the product rotation strongly aligned about the direction of the relative velocity of the reagent. Zhao et al. research the effect of reagent vibrational excitation and isotope substitution on the stereodynamics of $\text{Ba} + \text{HF} \rightarrow \text{BaF} + \text{H}$ [24], the results suggest that the vibrational excitation of reagent has a great influence on the differential cross sections. However, as a HHL mass system, the existing work on the reaction $\text{Ca} + \text{HCl}$ mainly focuses on the study of the scalar property [25], while there are few reports about the stereodynamics and the vibrational excitation effects of reagent.

With the rapid development of reaction dynamics during the past few decades [26–30], the stereodynamics of chemical reaction has attracted many people's attention. In order to understand the dynamics of the $\text{Ca} + \text{HCl}$ reaction fully, it is important to study not only their scalar properties, but also their vector properties. We utilize QCT method, which contains the sixth-order symplectic integrator [31], to study the stereodynamics of the title reaction. In particular, the influence of the reagent vibration on the $\text{Ca} + \text{HCl}$ ($v = 0-2, j = 0$) reaction is analyzed.

* Corresponding author. Tel./fax: +86 535 6672870.

E-mail address: yangchuanlu@263.net (C.-L. Yang).

2. Computational methods

2.1. Quasi-classical trajectory calculations

The quasi-classical trajectory (QCT) program used for calculating the stereodynamic properties in this paper can be found in Refs. [31–35]. the classical Hamiltonians are numerically integrated in three dimensions, the accuracy of which is verified by checking the conservation of total energy and total angular momentum for every trajectory. A well-known drawback of the QCT method is its inability to properly treat quantum-mechanical effects, such as the zero-point-energy problem, resonance, tunneling, and non-adiabatic transitions. Many strategies have been proposed to approximate the zero-point energy but no satisfactory procedure has emerged. Here, a passive method of discarding all reactive trajectories forming products with a total vibrational energy lower than the total harmonic zero-point energy of the products is employed. Therefore, the QCT treatment of the reactions is sufficiently accurate.

In the calculations, batches of 10^5 trajectories are run for each reaction and the integration step size is chosen as 0.1 fs. The collision energy is chosen as 0.8 eV for the title reactions. The accuracy of the numerical integration is verified by checking the conservation of the total energy and total angular momentum for every trajectory. The vibrational and rotational levels of the reactants molecules are taken as $v = 0, 1, 2$ and $j = 0$, respectively. The trajectories start at an initial distance of 15.0 Å between the Ca atom and the center of mass of HCl. The impact parameters b_{max} for the three reactions of $\text{Ca} + \text{HCl}$ ($v = 0-2, j = 0$) on PES are 2.0/2.8/3.3 Å, respectively.

2.2. Rotational polarization of product

The computational formulae of the rotational polarization of the product can be found elsewhere [34–37]; here we will only present the definitions of the vectors in brief. In the center-of-mass (CM) frame, we choose the center-of-mass (CM) frame shown in Fig. 1 to express the degree of the polarization of product rotational angular momentum \vec{j} . The reagent relative velocity vector \vec{k} is parallel to the z-axis and x–z plane is the scattering plane containing the initial and final relative velocity vectors, \vec{k} and \vec{k}' , θ_t is the angle between \vec{k} and \vec{k}' , θ_r and ϕ_r are the polar and azimuthal angles of the final rotational angular momentum \vec{j} , respectively.

The distribution function $P(\theta_r)$ describing the \vec{k} – \vec{j} correlation can be expanded in a series of Legendre polynomials. The expanding coefficients are called orientation (k is odd) or alignment (k is even) parameters. The dihedral angle distribution function $P(\phi_r)$

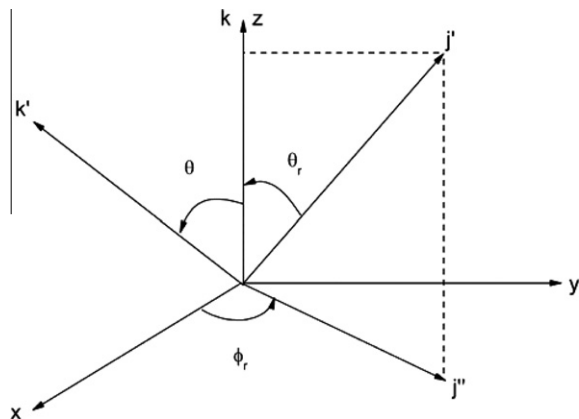


Fig. 1. The center-of-mass coordinate system to describe the \vec{k} , \vec{k}' and \vec{j} correlations.

describing \vec{k} – \vec{j} correlation can be expanded in Fourier series. $P(\theta_r)$, $P(\phi_r)$ and $P(\theta_r, \phi_r)$ is expanded up to $k = 18, 24, 7$, respectively, which shows good convergence.

The fully correlated CM angular distribution is written as

$$P(\omega_t, \omega_r) = \sum_{kq} \frac{(2k+1)}{4\pi} \frac{1}{\sigma} \frac{d\sigma_{kq}}{d\omega_t} C_{kq}(\theta_r, \phi_r)^* \quad (1)$$

where $(1/\sigma)(d\sigma_{kq}/d\omega_t)$ is a generalized polarization-dependent differential cross-section (PDDCS). The PDDCS is written in the following form,

$$\frac{1}{\sigma} \frac{d\sigma_{kq\pm}}{d\omega_t} = \sum_{k_1} \frac{k_1}{4\pi} S_{kq\pm}^{k_1} C_{k_1q}(\theta_t, 0) \quad (2)$$

where the $S_{kq\pm}^{k_1}$ is evaluated using the expected value expression

$$S_{kq\pm}^{k_1} = \langle C_{k_1q}(\theta_t, 0) C_{kq}(\theta_r, 0) [(-1)^q e^{iq\phi_r} \pm e^{-iq\phi_r}] \rangle \quad (3)$$

where the angular brackets represent an average over all angles. Many photon-initiated bimolecular reaction experiments will be sensitive to only those polarization moments with $k = 0$ and $k = 2$. In order to compare calculations with experiments, $(2\pi/\sigma)(d\sigma_{00}/d\omega_t)$, $(2\pi/\sigma)(d\sigma_{20}/d\omega_t)$, $(2\pi/\sigma)(d\sigma_{22+}/d\omega_t)$, $(2\pi/\sigma)(d\sigma_{21-}/d\omega_t)$ are calculated. In the above calculations, PDDCSs are expanded up to $k_1 = 7$, which is sufficient for good convergence.

2.3. Characteristics of the PES

In our calculation, the PES we used was constructed by Verbockhaven et al. [22], which describes the full reaction from $\text{Ca}(4s^2, ^1S) + \text{HCl}$ reactants to $\text{Ca}(X^2\Sigma) \text{Cl} + \text{H}$ products. This surface is based on accurate *ab initio* calculations at the MRCI level, two fit procedures were applied by analytical functions: A fit to the complete set of 6400 *ab initio* energies points computed by MRCI on the global grid, and a local fit in the region of the van der Waals well to the extra points calculated in the entrance channel. This local fit was applied both to the MRCI and CCSD (T) results and it was used to check the accuracy of the global fit in the weak-interaction region.

The PES was used to perform quantum reactive-scattering calculations for the collision energy range of 0.2–1.0 eV by Sanz et al. [25], the reliability of the PES is confirmed by comparing the computational results with recent experimental values.

3. Results and discussion

Fig. 2 shows the calculated $P(\theta_r)$ distribution of product from the reaction $\text{Ca} + \text{HCl}$ ($v = 0-2, j = 0$) $\rightarrow \text{CaCl} + \text{H}$ at a collision energy of 0.8 eV, respectively. The distribution of $P(\theta_r)$ represents the \vec{k} – \vec{j} correlation. It is obviously that peak of the $P(\theta_r)$ distributions is at $\theta_r = 90^\circ$ and symmetric with regard to 90° , which directly demonstrates that the product rotational angular momentum vector \vec{j} is strongly aligned along the direction perpendicular to the relative velocity direction \vec{k} . It is obvious that the excitation of the initial HCl vibration has an obvious impact on the stereodynamics. From the plot, we can see that the alignment of product CaCl changes dramatically when the HCl molecule vibrations are excited to the $v = 1, 2$. The peak of $P(\theta_r)$ becomes higher when the reagent vibration $v = 1, 2$, indicating that the product rotational alignment effect becomes stronger when the reagent is in the excited vibration states. This may be explained from the expectation values of $P_2(\cos\theta)$ which are -0.496183 , -0.498012 and -0.498345 , respectively. As we know, $\langle P_2(\cos\theta) \rangle$ is very important because when the values are close to -0.5 , suggesting that \vec{j} is preferentially polarized and perpendicular to the reagent relative velocity. Some more detailed explanations are presented in the following, the reaction is

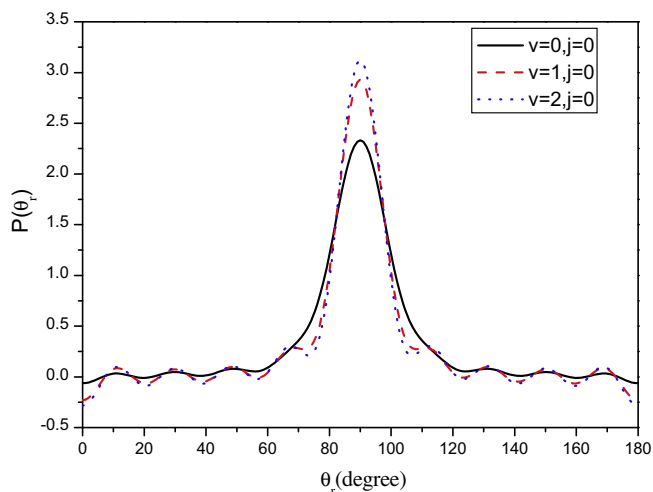


Fig. 2. The angular distribution of $P(\theta_r)$ reflecting the $\mathbf{k}-\mathbf{j}'$ correlation is shown for the three reactions. Solid line indicates $\text{Ca} + \text{HCl} (v=0, j=0) \rightarrow \text{CaCl} + \text{H}$; dashed line indicates $\text{Ca} + \text{HCl} (v=1, j=0) \rightarrow \text{CaCl} + \text{H}$; dotted line indicates $\text{Ca} + \text{HCl} (v=2, j=0) \rightarrow \text{CaCl} + \text{H}$.

mainly direct reaction, while the CaCl molecule produces and the bond between H and Cl breaks, the H atom will impact effect on the vibrational and rotational status of the CaCl molecule. However, the effect should become weaker when the molecule HCl is in the excited vibration states because the bound between H and Cl gets weaker. Therefore, the product rotational alignment effect of CaCl becomes stronger when the reagent molecule HCl is in the excited vibration states.

Fig. 3 shows the distributions of the dihedral angle distribution of $P(\phi_r)$ which describes the correlation of $\mathbf{k}-\mathbf{k}'-\mathbf{j}'$. $P(\phi_r)$ tends to be asymmetric with respect to the $\mathbf{k}-\mathbf{k}'$ scattering plane (or about $\phi_r = 180^\circ$), directly reflecting the strong polarization of the angular momentum. Those peaks appear at $\phi_r = 90^\circ$ and 270° , showing that the \mathbf{j}' of products of the three reactions are mainly aligned along the y -axis of the CM frame. For each reaction, the peak at $\phi_r = 270^\circ$ is evidently higher than that at $\phi_r = 90^\circ$ reveals that the rotational angular momentum vector of product CaCl is not only aligned but also oriented along the negative direction of y -axis. With the increase of reagent vibrational quantum number,

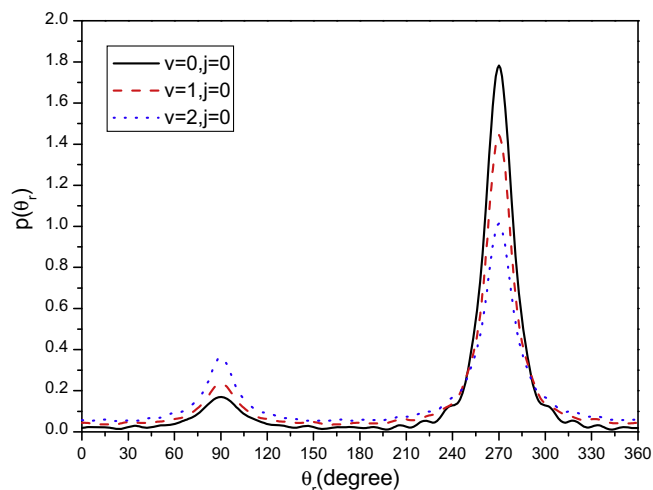


Fig. 3. The angular distribution of $P(\phi_r)$ with respect to the $\mathbf{k}-\mathbf{k}'$ plane. Solid line indicates $\text{Ca} + \text{HCl} (v=0, j=0) \rightarrow \text{CaCl} + \text{H}$; dashed line indicates $\text{Ca} + \text{HCl} (v=1, j=0) \rightarrow \text{CaCl} + \text{H}$; dotted line indicates $\text{Ca} + \text{HCl} (v=2, j=0) \rightarrow \text{CaCl} + \text{H}$.

the peaks become higher and higher at $\phi_r = 90^\circ$ and the peaks become lower and lower at $\phi_r = 270^\circ$ indicating that the orientation along the negative direction of y -axis becomes unobvious as the v increases.

In order to obtain more information about the angular momentum polarization, the polar plots of $P(\theta_r, \phi_r)$ distribution averaged

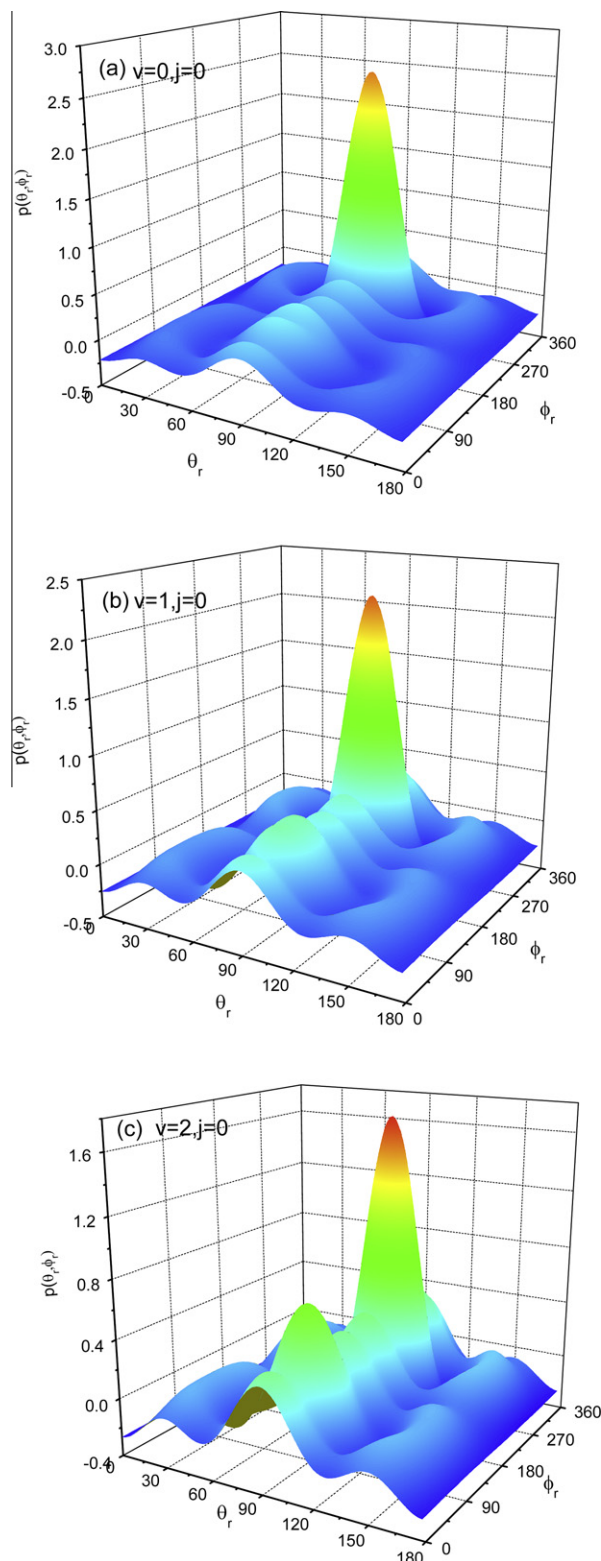


Fig. 4. Polar plots of $P(\theta_r, \phi_r)$ distribution averaged over all scattering angles. (a), (b) and (c) correspond to $\text{Ca} + \text{HCl} (v=0-2, j=0) \rightarrow \text{CaCl} + \text{H}$, respectively.

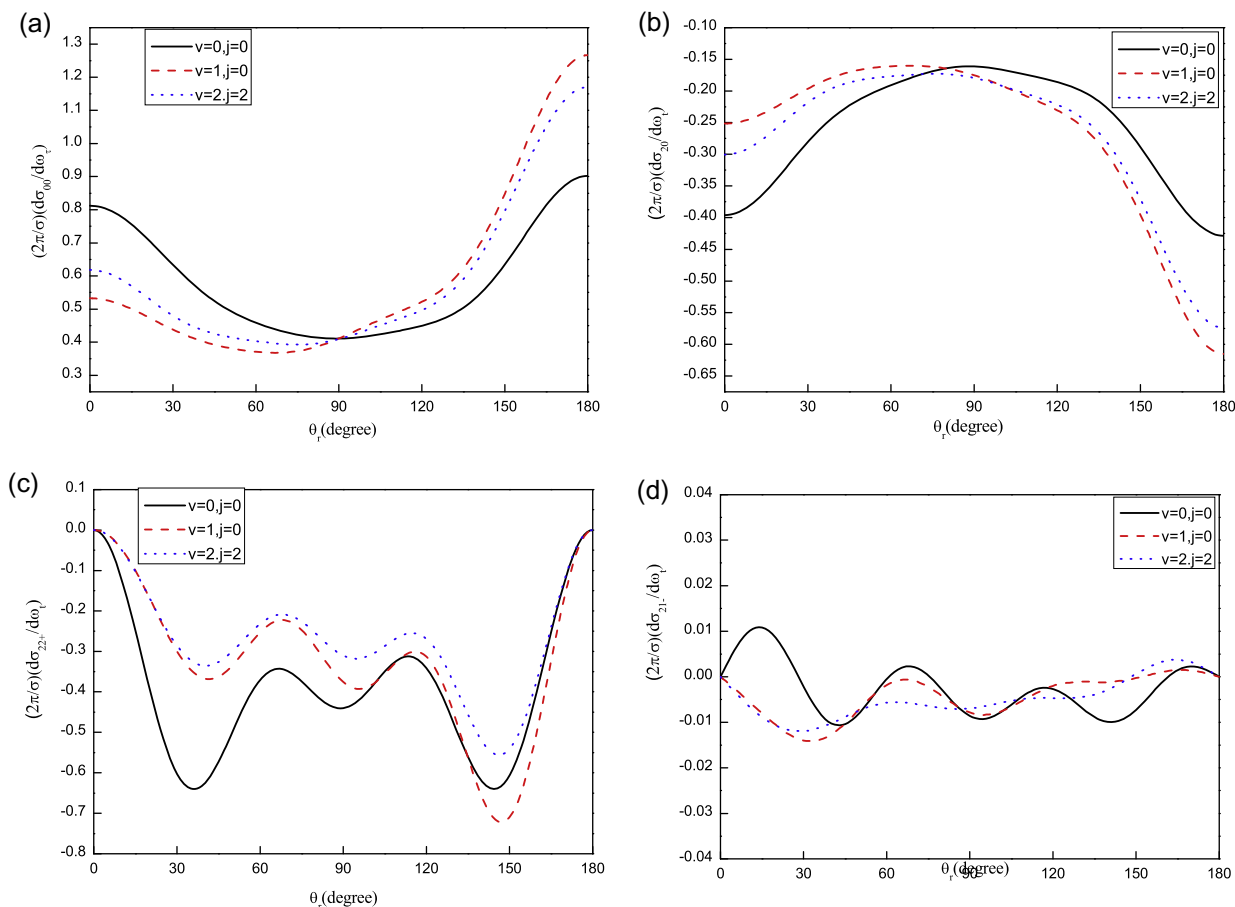


Fig. 5. (a) Shows the PDDCS with $(k, q) = (0, 0)$. Panels (b–d) depict the PDDCSs with $(k, q_{\pm}) = (2, 0), (2, 2+), (2, 1-)$ respectively.

over all scattering angles for the three reactions are given in Fig. 4. The distributions which peak at $(90^\circ, 270^\circ)$ and $(90^\circ, 90^\circ)$ are in good accordance with that of $P(\theta_r)$ and $P(\varphi_r)$. Furthermore, one can also conclude from the distribution of $P(\theta_r, \varphi_r)$ that the products are strongly polarized perpendicular to the scattering plane and the products of the reaction are mainly left-handed rotating in planes parallel to the scattering plane.

The polarization dependent generalized differential cross-sections (PDDCSs) describe the $\mathbf{k}-\mathbf{k}'-\mathbf{j}$ correlation and the scattering direction of the product molecule. The results of the reactions are shown in Fig. 5.

The PDDCS $(2\pi/\sigma)(d\sigma_{00}/dw_t)$, which is simply the differential cross-section (DCS), only describes the $\mathbf{k}-\mathbf{k}'$ correlation or the scattering direction of the product and is not associated with the orientation and alignment of the product rotational angular momentum vector \mathbf{j} , is shown in Fig. 5(a). The product molecule CaCl is strongly forward, backward scattering, and weakly sideways scattering for $\text{Ca} + \text{HCl}$ ($v = 0, j = 0$) reaction, there is no distinct scattering direction from forward scattering to backward scattering, while the reaction $\text{Ca} + \text{HCl}$ ($v = 1, 2, j = 0$) is governed by strong backward scattering. Therefore, one can conclude that the tendency of backward scattering is enhanced with the increase of vibrational quantum number of the reagent.

The PDDCS $(2\pi/\sigma)(d\sigma_{20}/dw_t)$ is the expectation value of the second Legendre moment of $\langle p_2(\cos \theta_r) \rangle$. The curves show the opposite trend to that of $(2\pi/\sigma)(d\sigma_{00}/dw_t)$, which indicates that \mathbf{j} is strongly aligned perpendicular to \mathbf{k} . The trend is especially obvious when $\theta_t = 180^\circ$, showing the preferential polarization along the direction perpendicular to \mathbf{k} at this angle. The trend

becomes stronger as the reagent molecular vibrates in $v = 1, 2$ states.

The PDDCS $(2\pi/\sigma)(d\sigma_{22+}/dw_t)$ is relative to $\langle \sin^2 \theta_r \cos 2\phi_r \rangle$, the distributions of which is depicted in Fig. 5(c). The values of $(2\pi/\sigma)(d\sigma_{22+}/dw_t)$ are negative indicating the remarkable preference of product alignment along the y-axis. The polarization trend of three reactions is displayed consistently, the strong polarization of the product for the three reactions appears at about $\theta_t = 38^\circ$ and $\theta_t = 145^\circ$.

The PDDCS $(2\pi/\sigma)(d\sigma_{21-}/dw_t)$, which is related to $\langle -\sin^2 \theta_r \cos \phi_r \rangle$, is depicted in Fig. 2(d). \mathbf{j} of CaCl tends to different distribution when the reagent molecular vibrates in different state reflecting that it is also affected by the reagent vibration.

4. Conclusion

In this paper, we have employed QCT method to investigate the effect of the reagent vibration on stereodynamics of the reaction $\text{Ca} + \text{HCl}$ ($v = 0-2, j = 0$) \rightarrow $\text{CaCl} + \text{H}$. The results demonstrate that the vibraional quantum number has a considerable influence on the distribution of the $\mathbf{k}-\mathbf{j}$ vector correlation, the alignment effect of products becomes stronger with the increase of vibrational quantum numbers. The rotational angular momentum vector \mathbf{j} of CaCl is not only aligned, but also oriented along the negative direction of y-axis. There also exists strongly forward and backward scattering and weakly sideways scattering as HCl is in vibration ground state, and preferred backward scattering as reagent is in $v = 1, 2$ vibration states. Furthermore, the PDDCSs are clearly influenced by the reagent vibration.

Acknowledgements

Many thanks should be given to Prof. Keli Han for providing stereodynamics QCT code. This work is supported by the National Science Foundation of China under Grant Nos. 10974078, 11174117, 1147026, 10874104.

References

- [1] J.L. Magee, J. Chem. Phys. 8 (1940) 687.
- [2] A. Mims, S.M. Lin, R.R. Hem, J. Chem. Phys. 57 (1972) 3099.
- [3] A. Torres-Filho, J.G. Pruett, J. Chem. Phys. 77 (1982) 1774.
- [4] H.W. Cruse, P.J. Dagdigian, R.N. Zare, Faraday Discuss. Chem. Soc. 55 (1973) 277.
- [5] J.G. Pruett, R.N. Zare, J. Chem. Phys. 64 (1976) 1774.
- [6] A. Gupta, D.S. Perry, R.N. Zare, J. Chem. Phys. 76 (1980) 237.
- [7] R.N. Zare, Faraday Discuss. Chem. Soc. 67 (1979) 7.
- [8] D. Feldman, R.K. Lengel, Chem. Phys. Lett. 52 (1977) 413.
- [9] M.Q. Cai, L. Zhang, B.Y. Tang, M.D. Chen, G.W. Yang, K.L. Han, Chem. Phys. 283 (2000) 255.
- [10] C. Noda, J.S. McKillop, M.A. Johnson, J.R. Waldeck, R.N. Zare, J. Chem. Phys. 85 (1986) 856.
- [11] D. Zhao, J. Chem. Phys. 97 (1992) 6208.
- [12] A.A. Tsekouras, C.A. Leach, K.S. Kalogerakis, R.N. Zare, J. Chem. Phys. 97 (1992) 720.
- [13] J.M. Teule, J. Mes, M.H.N. Jassen, S. Stolte, J. Chem. Phys. 856 (2000) 85.
- [14] R. Altkom, F.E. Bartoszek, J.D. Haven, G.C. Han, D.S. Perry, R.N. Zare, Chem. Phys. Lett. 98 (1983) 212.
- [15] Z. Karny, R.C. Estler, R.N. Zare, J. Chem. Phys. 69 (1969) 5199.
- [16] A. Gupta, D.S. Perry, R.N. Zare, J. Chem. Phys. 72 (1980) 6250.
- [17] Z. Karny, R.N. Zare, J. Chem. Phys. 68 (1978) 3360.
- [18] B. Soep, C.J. Whitham, A. Keller, J.P. Visticot, Faraday Discuss. Chem. Soc. 91 (1991) 191.
- [19] B. Soep, S. Abbès, A. Keller, J.P. Visticot, J. Chem. Phys. 96 (1992) 440.
- [20] A. Keller, R. Lawruszczuk, B. Soep, J.P. Visticot, J. Chem. Phys. 105 (1996) 4556.
- [21] J.P. Visticot, B. Soep, C.J. Whitham, J. Phys. Chem. 92 (1988) 4574.
- [22] G. Verbockhaven, C. Sanz, G.C. Groenenboom, O. Roncero, J. Chem. Phys. 122 (2005) 204307.
- [23] L.Z. Wang, C.L. Yang, J.J. Liang, J. Xiao, Q.G. Zhang, Chin. J. Chem. Phys. 24 (2011) 686.
- [24] J. Zhao, Y. Luo, Chin. Phys. B 4 (2011) 20.
- [25] C. Sanz, A. Avoird, O. Roncero, J. Chem. Phys. 123 (2005) 064301.
- [26] X.G. Liu, Q.G. Zhang, Y.C. Zhang, M.L. Wang, Chin. Phys. 13 (2004) 1013.
- [27] J.J. Liang, X.G. Lu, W.W. Xu, H. Kong, Q.G. Zhang, Theochem 942 (2010) 93.
- [28] J. Xiao, C.L. Yang, M.S. Wang, X.G. Ma, Chem. Phys. 379 (2011) 46.
- [29] J. Zhao, Y. Xu, Q.T. Meng, J. Phys. B 42 (2009) 165006.
- [30] Y. Xu, J. Zhao, D.G. Yue, H. Liu, Q.T. Meng, Chin. Phys. B 18 (2009) 5308.
- [31] X. Zhang, Int. J. Quant. Chem. 106 (2006) 1815.
- [32] M.D. Chen, N.Q. Lou, Chem. Phys. Lett. 357 (2002) 483.
- [33] M.L. Wang, K.L. Han, G.Z. He, J. Phys. Chem. A 102 (1998) 10204.
- [34] M.D. Chen, K.L. Han, N.Q. Lou, Chem. Phys. 283 (2002) 463.
- [35] M.D. Chen, K.L. Han, N.Q. Lou, J. Chem. Phys. 118 (2003) 4463.
- [36] F.J. Aoiz, M. Brouard, P.A. Enriquez, J. Chem. Phys. 105 (1996) 4964.
- [37] J.J. Ma, M.D. Chen, S.L. Cong, K.L. Han, Chem. Phys. 327 (2006) 529.